

ORIGINAL ARTICLE

The impact of composition, core metal mass and phase transformation behaviour on the dynamic cyclic fatigue of Ni-Ti files at different temperatures

ABSTRACT

Aim: To assess impact of elemental composition, core metal mass and phase transformation behaviour on the dynamic cyclic fatigue resistance of three Ni-Ti rotary files at room and body temperatures.

Methods: Twenty instruments of each system were tested for dynamic cyclic fatigue resistance in a simulated root canal with a 90° angle of curvature and a 5-mm radius of curvature at room and body temperature. The core metal mass at the fractured surface of each instrument was calculated by Image J software analysis of SEM images. The energy dispersive X-ray analysis was used to assess file composition. Scanning calorimetry was used to assess the structural phase state and the transformation temperature. One-way analysis of variance (ANOVA) was performed to determine any statistical difference amongst groups. For inter-group comparison, the unpaired t-test was used.

Results: HEDM showed significantly higher TtF and NCF values than AFBS and ZB-F6 instruments, at both temperatures tested. The mean core metal mass was smallest in HEDM followed by AFBS with no statistical difference between them, while ZB-F6 had the significantly largest metal core. EDX analysis showed that all the instruments were mainly composed by nickel and titanium. DSC analysis revealed that HEDM and AFBS exhibited a martensitic phase at body (37 °C) and room temperature (25 °C), whereas ZB-F6 revealed an austenitic phase at body temperature.

Conclusions: Dynamic cyclic fatigue resistance increased when the instruments had less cross-sectional metal mass, less Ni (wt%), a thermally treated surface, and a martensite phase at body temperature.

Mohamed Salah Abdel Aziz El-wakeel¹

Ahmed Abdel Rahman Hashem^{1*}

Sarah Hossam Fahmy¹

Shehabeldin Mohamed Saber^{1,2}

Gianluca Plotino³

¹Department of Endodontics, Faculty of Dentistry, Ain Shams University, Egypt

²Department of Endodontics, Faculty of Dentistry, and Center of Innovative Dental sciences, The British University, Egypt

³Grande Plotino & Torsello, Private Practice in Rome, Italy

Received 2022, February 21

Accepted 2022, May 2

KEYWORDS dynamic cyclic fatigue, differential scanning calorimetry, energy dispersive X-ray analysis, nickel-titanium instruments

Corresponding Author

Ahmed Abdel Rahman Hashem | Professor and Head of Endodontics Department, Faculty of Dentistry, Ain Shams University | Egypt.
Tel: +202-26401884 | Mobile: +20-1001040434 | Email: endohashem@gmail.com

Peer review under responsibility of Società Italiana di Endodonzia

[10.32067/GIE.2021.35.02.58](https://doi.org/10.32067/GIE.2021.35.02.58)

Società Italiana di Endodonzia. Production and hosting by Ariesdue. This is an open access article under the CC BY-NC-ND license (<http://creativecommons.org/licenses/by-nc-nd/4.0/>).

Introduction

Nickel-titanium (NiTi) instruments can shape root canals faster, with better-centered preparations and fewer procedural errors than stainless steel ones (1). Yet, unexpected instrument fracture still does occur. Two modes of fracture were identified by Sattapan et al. (1), torsional and fatigue failures. Fracture due to torsion occurs upon reaching the ultimate shear strength of the file, while cyclic fatigue is attributed to metal fatigue when it rotates freely in a curved canal at the point of maximum flexure (2, 3). Several factors contribute to the cyclic fatigue resistance of NiTi instruments, including operational settings, alloy composition, metallurgical properties, and the thermo-mechanical history of the instrument (1-5). Recent studies have shown that environmental temperature during testing also influences the cyclic fatigue failure of NiTi instruments (6, 7). As instrument fracture could jeopardize the outcome of endodontic treatment, it is essential to understand the impact of elemental composition and structural phase state on the fatigue resistance of NiTi endodontic files, especially in a dynamic model and a simulated body temperature.

The present study aimed to study the impact of elemental composition, core metal mass and phase transformation behaviour on the dynamic cyclic fatigue resistance of Hyflex EDM One file (COLTENE/Whaledent, Altstätten, Switzerland), (HEDM), AF blue S one (Fanta Dental Materials Co. Ltd., Shanghai, China) (AFBS) and ZB-F6 Ni-Ti rotary files (Foshan Qiyang Medical Equipment Limited, Guangdong, Guangdong, China) at room and simulated body temperatures. The null hypotheses tested were that there would not be significant differences among the instruments regarding their cyclic fatigue resistance and that cyclic fatigue is not influenced by the testing temperature.

Materials and Methods

Sample size calculation

A statistical sample size calculation was performed using the G-power program based on a previous study. An alpha-type error of 0.05, a beta power of 0.95, and an N2/N1 ratio of 1.

Dynamic cyclic fatigue test

Twenty new instruments with tip sizes (#25) from three NiTi rotary systems, HyFlex EDM OneFile (HEDM), AF Blue S One (AFBS), and ZB-F6 were tested at room

Figure 1
Cyclic fatigue assembly:
A) custom-made dynamic cyclic fatigue device; **B)** custom-made water bath; **C)** endodontic motor; **D)** screen display of the code responsible for dynamic movement; **E)** Arduino/CNC shield complex.

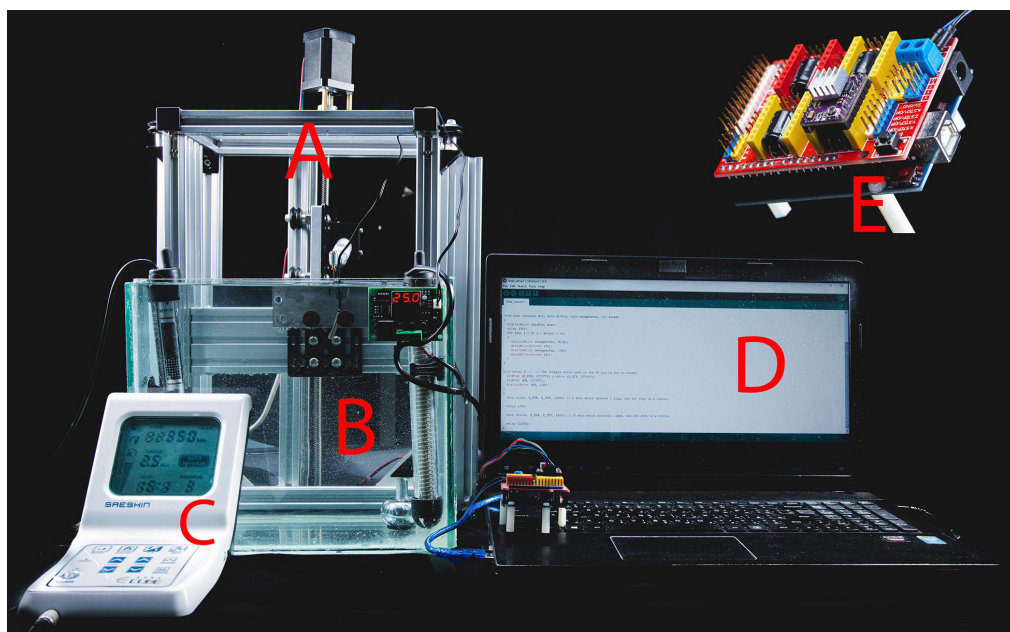
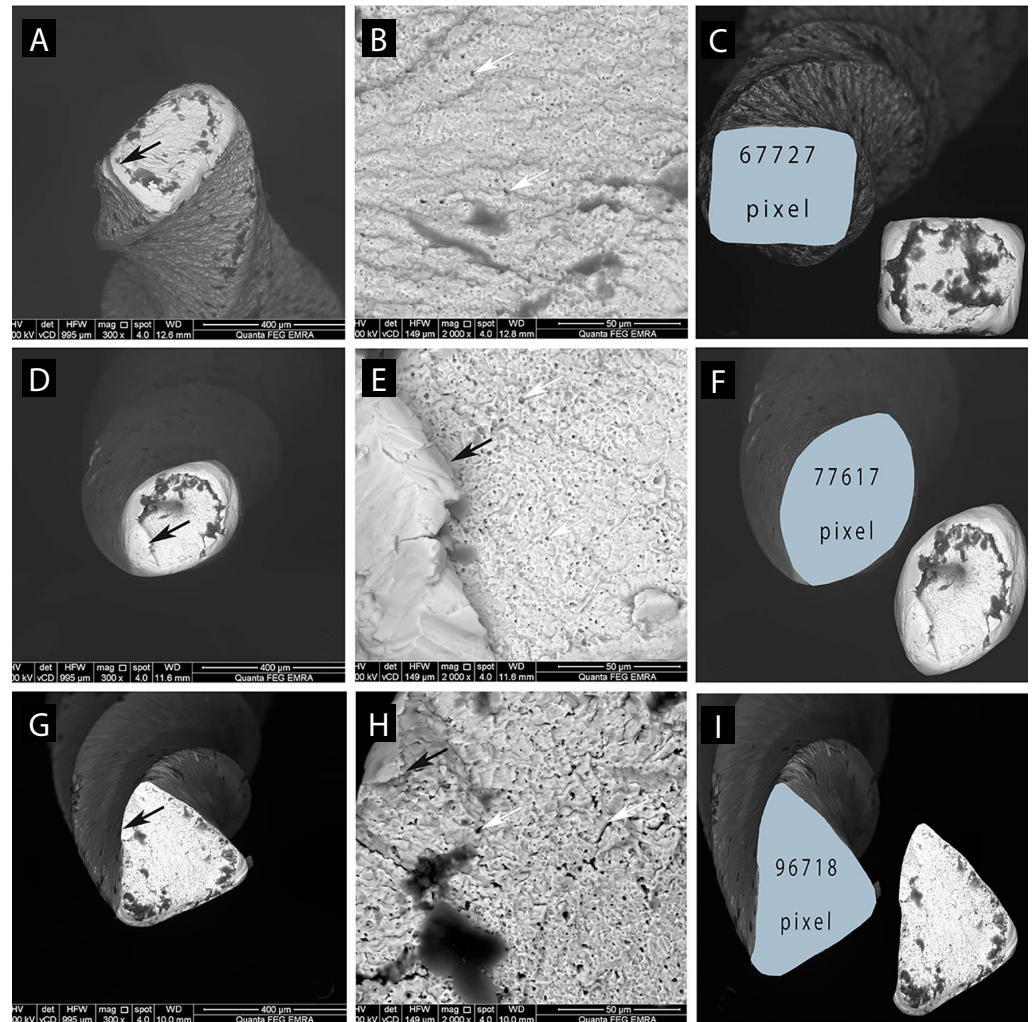


Figure 2
SEM photomicrographs of the fractured surface after cyclic fatigue testing. General view of HEDM (A), AFBS (D) and ZB-F6 (G); instruments showing area of elevation (black arrows), and high-magnification view of HEDM (B), AFBS (E) and ZB-F6 (H); instruments showing microstructure voids (white arrows), both typical signs of ductile failure. And (x500) used to determine the amount of metal mass (in pixels) at the level of the instrument fracture for of HEDM (C), AFBS (F) and ZB-F6 (I).



temperature (25 °C, $n=10$) and body temperature (37 °C, $n=10$). Instruments were operated according to the manufacturer's instructions in a simulated stainless-steel canal (tip size #25/0.08 taper +0.2 mm offset) using a 16:1 reduction handpiece (Saeshin Precision Co., Ltd, Korea). The simulated root canal was 16 mm long with a 90° angle of curvature and a 5mm radius of curvature according to Pruett's method (8). The straight segment of the canal was 11 mm and the center of curvature was 5 mm away from the instrument tip. A new custom-made device was designed (Egyptian patent number 265/2021) and constructed to be used for dynamic cyclic fatigue testing in the present study (Figure 1). The device is composed of a custom-made linear actuator attached to a custom-made frame holding the handpiece

and the artificial canal. The linear actuator is connected to a CNC shield/Arduino Uno complex (Arduino. cc, USA).

A custom code written by the Arduino software (version 1.8.13, Arduino.cc, USA) controlled the magnitude of the vertical distance and time (1.5 mm/0.5 s upwards and 1.5 mm/0.5 s downwards) of the rotating file. The code allowed repeatable cycles with a 1 second relay. Both the device and the endodontic motor were started simultaneously. The auto-reverse mode of the endodontic motor was turned off. The cyclic fatigue apparatus was inserted in a custom-made water bath with a heat controller to regulate the desired testing temperature. The test was performed two times for each group, one at room temperature 25 °C ± 0.5 °C and the other at body temperature 37 °C ± 0.5 °C. A video was cap-



Figure 3
DSC analysis, showing heating and cooling curve with phase transformation temperatures for each file.

tured and time to fracture (T_{tf}) was evaluated frame by frame using a special video editing program (Adobe Premiere Pro 2020, Adobe Inc, USA), recorded and tabulated for all groups. The number of cycles to fracture (NCF) was then calculated and the

fractured fragment length (FL) was measured in mm unit for each instrument tested.

Fractographic and metal mass examination by scanning electron microscope (SEM)

**Table 1**

Time to fracture (seconds), number of cycles to failure, fragment length (mm), metal mass (pixels), the Predicted cycles for 99% survival and correlation coefficient for the different instruments at the different tested temperatures

	TtF		NCF		Fragment length		Metal mass in pixels	Predicted cycles for 99% survival		Correlation coefficient	
	25 °C	37 °C	25 °C	37 °C	25 °C	37 °C		25 °C	37 °C	25 °C	37 °C
HEDM	40.0160 ±0.0389 ^a	39.9170 ±0.2068 ^a	266.773 ±0.260 ^a	266.113 ±1.378 ^a	3.18 ±0.092 ^a	3.18 ±0.123 ^a	68727 ±2006 ^a	269.072	268.329	0.944	0.829
AFBS	38.8290 ±0.0706 ^b	38.7760 ±0.0517 ^b	258.860 ±0.471 ^b	258.505 ±0.345 ^b	3.15 ±0.108 ^a	3.17 ±0.095 ^a	78617 ±2568 ^a	261.091	260.650	0.957	0.874
ZB-F6	8.0360 ±0.0331 ^c	5.8460 ±0.1166 ^c	52.5733 ±0.220 ^c	38.974 ±0.778 ^c	3.26 ±0.108 ^a	3.25 ±0.151 ^a	97828 ±3190 ^b	54.0347	39.1740	0.984	0.957

Different superscript letters in the same column were statistically significant ($p < 0.05$).

The values are means \pm standard deviations.

TtF: time to fracture, NCF: number of cycles to fracture, metal mass and fractured fragment length.

All fractured instruments were examined by SEM (Philips SEM 515, Eindhoven, Netherlands). The broken fragments were ultrasonically cleaned in absolute ethyl alcohol for approximately ten minutes before analysis at 500x and 2000x magnification at 25 kV and room temperature to evaluate the type of fracture. The 500x SEM images were analyzed using Image J software (Image J, USA) to determine the amount of metal mass of each file in pixels at the fracture level (Figure 2).

Elemental analysis by energy-dispersive X-ray (EDX) analysis

The surfaces of three new instruments from each brand were analyzed to evaluate their chemical composition by EDX analysis using a field emission SEM (FEI Company, Hillsboro, Oregon-USA). Samples were mounted onto SEM stubs and analyzed at a 10.1 mm working distance, with an in-lens detector and an excitation voltage of 20 kV.

Phase transformation behaviour by differential scanning calorimetry (DSC)

Four new instruments from each file system were evaluated using DSC (Diamond Dsc, PerkinElmer, Waltham, USA) with scans ranging from approximately 65 °C to -5 °C to assess the metallurgical phase of the

file at different temperatures (4 °C, 25 °C, 37 °C) and transformation temperatures. Two different tests on two new instruments from each system were conducted, aiming the second to confirm the result of the first one.

Statistical analysis

The Shapiro-Wilk and Levene test was used to evaluate the assumption of normality and the equality of variance of the data sets. Considering that the dynamic cyclic fatigue resistance results were normally distributed ($P > 0.05$), they were presented as mean and standard deviation values of TtF, NCF, FL, and metal mass. These results were analyzed using one-way analysis of variance (ANOVA) and Tukey Honestly Significant Difference (HSD) tests using Minitab 19 program (version 19, Minitab, LLC, USA) to determine any statistical difference amongst groups. For inter-group comparison, the unpaired *t*-test was used. In the present study, $P \leq 0.05$ was considered as the level of significance. Pearson correlation test was conducted with confidence level 95 to correlate metal mass, Ni (Wt%), and Af temperature with TtF.

Using Weibull reliability analysis, the probability for survival was calculated and charted in a reliability plot the steepness of the slope evaluated which represents the

Table 2

EDX analysis showing the mean Wt% ± standard deviations of each element of the three tested files

Element	HEDM	AFBS	ZB-F6
C	19.328±1.294	8.874±1.247	10.815±1.449
O	18.995±0.516	12.474±0.392	4.160±0.913
AL	3.447±0.379	3.440±0.403	4.308±1.205
Si	0.5600±0.0283	-	-
Ti	32.047±0.495	32.998±1.251	35.730±0.939
Ni	41.297±1.889	41.138±1.519	44.710±1.568

C: carbon, O: oxygen, AL: aluminium, Si: silicon, Ti: titanium, Ni: nickel.

Beta value. The correlation coefficient was calculated. The predicted maximum cycles for 99% probability of survival were calculated.

Results

Mean TtF and NCF after dynamic cyclic fatigue testing for all the instruments tested are displayed in Table 1. One-way ANOVA revealed a significant difference among the three tested instruments (P<0.05). HEDM showed the highest resistance to cyclic fatigue followed by AFBS and ZB-F6 files at both room and body temperatures (P<0.05). A significant difference was observed between body temperature and room temperature for the ZB-F6 file only (P>0.05). The length of all fractured segments showed no significant difference among all tested groups denoting accurate device trajectory.

Weibull probability plots (reliability Vs time) per group revealed that the ZB-F6 file has the lowest Beta value among the tested groups at body temperature. The Predicted cycles for 99% survival, the correlation coefficient is represented in (Table 1). HEDM at room temperature showed the highest predicted number of cycles to fracture for 99% survival by 269.072 cycles while ZB-F6 at body temperature showed the lowest predicted number of cycles to fracture for 99% survival by 39.174 cycles.

All groups showed a correlation coefficient higher than 0.75.

The fractographic examination confirmed a predominantly ductile mode of fracture for all tested instruments, typical for fractures due to accumulation of metal fatigue (Figure 2). This was evident by areas of elevations at the peripheries at high magnification and dimpled surfaces at low magnification. The dimpled surfaces revealed different characteristics for each instrument type: for HEDM and AFBS instruments, the dimples were fewer and relatively smaller, while for ZB-F6 instruments the dimples were larger and more numerous. The metal mass calculation (Table 1) revealed that the mean core metal mass was smallest in HEDM (68727±2006) followed by AFBS (78617±2568) with no statistical difference between them (p>0.05), while ZB-F6 had the significantly largest metal core (9782± 3190) (p<0.05).

EDX analysis (Table 2) showed that all the instruments were mainly composed of nickel, titanium with slightly different percentages depending on the instrument tested.

Regarding the phase transformation behaviour, all tested brands showed a DSC curve with a single exothermic peak at cooling and a single endothermic peak at heating at the examined temperature range (Figure 3). The exothermic peaks represented the martensitic phase changes for AFBS



and ZB-F6 and the R-phase change for HEDM instruments, while the endothermic peaks represented the austenitic phase changes for all instruments. Martensitic start and finish temperatures and austenitic start and finish temperatures are listed in (Table 3). HEDM and AFBS files displayed a higher Af (53.505 ± 0.375 , 45.62 ± 2.376) than the body temperature. In comparison, ZB-F6 showed a lower Af (26.44 ± 0.523) than the body temperature. Pearson's correlation test showed a negative correlation between TtF and metal mass (-0.953) and Ni Wt% (-0.996) and a positive correlation with Af temperature (0.953).

Discussion

The present study evaluated the impact of elemental composition, core metal mass and phase transformation behaviour on of the dynamic cyclic fatigue resistance of Hyflex EDM One file (HEDM), AF blue S one (AFBS), and ZB-F6 Ni-Ti rotary files at room and simulated body temperatures. Recent studies advocated the simulation of clinical conditions during cyclic fatigue testing (6-11). The present study used a computer-guided novel dynamic model that allowed a pecking motion of 1.5 mm in both directions and can be operated in a water bath with simulated body temperature. It has an advantage over former dynamic models operated by universal testing machines or custom-made devices that

cannot be used in a water bath (12, 13). Results of the present study showed that HEDM files reported the highest cyclic fatigue resistance followed by AFBS and ZB-F6 files respectively, at both room and body temperatures. ZB-F6 showed the lowest cyclic fatigue at both temperatures ($P < 0.05$). This can be attributed to the thermomechanical processing treatment of the instruments during manufacturing. HEDM undergoes electric discharge machining which is a noncontact thermal erosion process that partially melts and evaporates the NiTi wire by high-frequency spark discharges. This technique was proved to enhance the mechanical properties greatly through reducing the surface defects and decreasing stresses on the instrument (13-15). The manufacturer of AFBS instruments claims instead a flowless surface finishing with a titanium oxide surface treatment that contributes to a better fatigue resistance (<http://www.fanta-dental.com/static/upload/file/20211101/1635745409400497.pdf>). This agrees to former studies highlighting the positive impact of heat treatment to reduce and correct machining defects (15, 16). The low cyclic fatigue resistance of ZB files can be attributed to the absence of such treatments.

The Weibull cumulative distribution function, which appears as a straight-line where the beta parameter is the slope of the line, indicated that ZB-F6 file showed the lowest predictability among the tested groups. The

Table 3
Phase transformation temperatures and enthalpy changes (ΔH)

	M_s ($^{\circ}C$)	M_f ($^{\circ}C$)	ΔH (j^{-1})	R_s ($^{\circ}C$)	R_f ($^{\circ}C$)	ΔH (j^{-1})	A_s ($^{\circ}C$)	A_f ($^{\circ}C$)	ΔH (j^{-1})
HEDM				44.41 ± 0.509	35.875 ± 0.332	1.1862 ± 0.568	43.03 ± 0.537	53.505 ± 0.375	2.549 ± 0.438
AFBS	38.33 ± 1.004	33.825 ± 0.757	41.17 ± 1.853				41.17 ± 1.853	45.62 ± 2.376	2.265 ± 0.529
ZB-F6	19.265 ± 0.177	15.28 ± 0.057	1.913 ± 0.446				21.305 ± 0.516	26.44 ± 0.523	2.265 ± 0.529

The values are means \pm standard deviations.

A_s : austenitic start, A_f : austenitic finish, M_s : martensitic start, M_f : martensitic finish, R_s : R-phase start, R_f : R-phase finish.



steeper the slope (beta), the smaller the variation in the time to failure and the more predictable the results will be. The correlation coefficient, which is the degree of the relation between the probability of survival and the predicted maximum cycles for each instrument, was higher than 0.75 for all files, which indicates a strong correlation.

Examination of the fractured instruments showed that they all fractured at the level of D3 to D4. At this level, HEDM has a quadratic cross-section and an 8% taper, the AFBS has an almost oval cross-section and 4% taper, while the ZB-F6 has a triangular cross-section and a 4% taper. Using Image J software (Image J, USA), the metal mass was calculated at the fracture level revealing that ZB-F6 files showed the largest metal mass that would explain the lower cyclic fatigue resistance obtained by the results of the study. Although the significant influence of cross-sectional design on the fatigue resistance had been reported by some studies (17, 18), other studies found that the cross-sectional design and the core size did not influence the fatigue resistance of Ni-Ti instruments (19, 20).

EDX analysis showed that the principal element in all files was nickel, 41.2 wt% for the HEDM instruments, 41.1 wt% for the AFBS instruments, and 44.7 wt% for the ZB-F6 instruments. It has been reported that the Ni content of a NiTi alloy influences the mechanical properties of endodontic instruments (20) which exhibit a lower percent in weight of nickel (52 Ni %wt. With the reduction of the Ni content, there is an increased tendency to obtain stable martensite, which is more flexible than austenite, at the working temperature (21). This finding is consistent with the results obtained in the present study by the mechanical dynamic cyclic fatigue test.

It has been postulated that the fatigue life of NiTi files was sensitive to the test environment (6, 22). Therefore, this study sought to compare the dynamic cyclic fatigue test at both room and simulated body temperatures. Theoretically, heat treatment is done during file manufacturing to increase the austenitic transformation finish temperature above the intracanal temperature. This

would help increase the fatigue life of the file (23). DSC analysis showed that the austenitic transformation of both HEDM and AFBS was above body temperature, while for ZB-F6 it was below body temperature. Moreover, HEDM showed an R-phase transformation around 37 °C, consistent with the previous studies (24-26) Cuyahoga Falls, OH [#25/08, manufactured by electrical discharge machining]. This explains the superior fatigue resistance of HEDM and AFBS over ZB-F6 instruments. Transformation of ZB-F6 to the austenitic phase below room temperature might also explain the difference observed in its cyclic fatigue resistance between the simulated room and body temperatures.

According to the results of the present study, both null hypotheses are rejected. HEDM and AFBS had significantly better fatigue resistance than ZB-F6 instruments and the fatigue life of ZB-F6 instruments was influenced by the testing temperature. Recently, the scientific value of studies on the fatigue resistance of rotary and reciprocating NiTi instruments has been questioned because of the large variability of the tested protocols, in absence of standardized specifications, that would make a comparison among studies difficult and problematic (27). It was also pointed out that this type of research does not resemble the reality because pure rotation inside an artificial canal without any torque on the instrument, such as in cyclic fatigue tests, was unlikely to happen in a clinical scenario. Although these statements are true, it is important to emphasize that cyclic fatigue and torsional resistance tests allow the variables to be isolated and tested individually, increasing the internal validity and reproducibility of the study, which agrees with basic concepts of the scientific method (28). Well-designed studies are warranted to evaluate the claims of the manufacturers and rank different generations of NiTi instruments.

Conclusions

Dynamic cyclic fatigue resistance of the rotary NiTi instruments tested increased when the instruments had less cross-section



tional metal mass, less Ni (wt%), a thermally treated surface, and a martensite phase at body temperature.

Clinical Relevance

The present study demonstrated clinical relevance for testing the resistance to cyclic fatigue of three instruments and thus making the root canal exploration with rotary instruments safer.

Conflict of Interest

Authors deny any conflict of interest.

Acknowledgments

None

References

- Sattapan B, Nervo GJ, Palamara JE, Messer HH. Defects in rotary nickel-titanium files after clinical use. *J Endod* 2000;26:161-5.
- Pruett JP, Clement DJ, Carnes DLJ. Cyclic fatigue testing of nickel-titanium endodontic instruments. *J Endod* 1997;23:77-85.
- Gambarini G, Seracchiani M, Piasecki L, et al. Measurement of torque generated during intracanal instrumentation in vivo. *Int Endod J* 2019;52:737-45.
- Saber SE. Factors influencing the fracture of rotary nickel titanium instruments. *ENDO* 2008;2:273-83.
- Ounsi HF, Al-Shalan T, Salameh Z, et al. Quantitative and qualitative elemental analysis of different nickel-titanium rotary instruments by using scanning electron microscopy and energy dispersive spectroscopy. *J Endod* 2008;34:53-5.
- de Vasconcelos RA, Murphy S, Carvalho CAT, et al. Evidence for reduced fatigue resistance of contemporary rotary instruments exposed to body temperature. *J Endod* 2016;42:782-7.
- Dosanji A, Paurazas S, Askar M. The effect of temperature on cyclic fatigue of nickel-titanium rotary endodontic instruments. *J Endod* 2017;43:823-6.
- Keleş A, Eymirli A, Uyanik O, Nağas E. Influence of static and dynamic cyclic fatigue tests on the lifespan of four reciprocating systems at different temperatures. *Int Endod J*. 2019;52:880-6.
- Pedullà E, Lo Savio F, Boninelli S, et al. Torsional and cyclic fatigue resistance of a new nickel-titanium instrument manufactured by electrical discharge machining. *J Endod* 2016;42:156-9.
- Pedullà E, La Rosa GRM, Virgillito C, et al. Cyclic fatigue resistance of nickel-titanium rotary instruments according to the angle of file access and radius of root canal. *J Endod* 2020;46:431-6.
- Hülsmann M, Donnermeyer D, Schäfer E. A critical appraisal of studies on cyclic fatigue resistance of engine-driven endodontic instruments. *Int Endod J* 2019;52:1427-45.
- Elsewify T, Saber S, Plotino G. Cyclic fatigue resistance of three heat-treated nickel-titanium instruments at simulated body temperature. *Saudi Endod J* 2020;10:131-6.
- Nishjo M, Ebihara A, Tokita D, et al. Evaluation of selected mechanical properties of NiTi rotary glide path files manufactured from controlled memory wires. *Dent Mater J* 2018;37:549-54.
- Özyürek T, Gündoğar M, Uslu G, et al. Cyclic fatigue resistances of Hyflex EDM, WaveOne gold, Reciproc blue and 2shape NiTi rotary files in different artificial canals. *Odontology* 2018;106:408-13.
- Tanomaru-Filho M, Espir CG, Venção AC, et al. Cyclic fatigue resistance of heat-treated nickel-titanium instruments. *Iran Endod J* 2018;13:312-7.
- Gündoğar M, Özyürek T. Cyclic fatigue resistance of OneShape, HyFlex EDM, WaveOne Gold, and Reciproc Blue nickel-titanium instruments. *J Endod* 2017;43:1192-6.
- Grande NM, Plotino G, Pecci R, et al. Cyclic fatigue resistance and three-dimensional analysis of instruments from two nickel-titanium rotary systems. *Int Endod J* 2006;39:755-63.
- Craveiro de Melo MC, de Azevedo Bahia MG, Lopes Buono VT. Fatigue resistance of engine-driven rotary nickel-titanium endodontic instruments. *J Endod* 2002;28:765-9.
- Cheung GSP, Darvell BW. Low-cycle fatigue of NiTi rotary instruments of various cross-sectional shapes. *Int Endod J* 2007;40:626-32.
- Testarelli L, Plotino G, Al-Sudani D, et al. Bending properties of a new nickel-titanium alloy with a lower percent by weight of nickel. *J Endod* 2011;37:1293-5.
- Zhou H, Shen Y, Zheng W, et al. Mechanical properties of controlled memory and superelastic nickel-titanium wires used in the manufacture of rotary endodontic instruments. *J Endod* 2012;38:1535-40.
- Huang X, Shen Y, Wei X, Haapasalo M. Fatigue resistance of nickel-titanium instruments exposed to high-concentration hypochlorite. *J Endod* 2017;43:1847-51.
- de Hemptinne F, Slaus G, Vandendael M, et al. Intracanal temperature evolution during endodontic treatment after the injection of room temperature or preheated sodium hypochlorite. *J Endod* 2015;41:1112-5.
- Arias A, Macorra JC, Govindjee S, Peters OA. Correlation between temperature-dependent fatigue resistance and differential scanning calorimetry analysis for 2 contemporary rotary instruments. *J Endod* 2018;44:630-4.
- Shen Y, Zhou HM, Zheng YF, et al. Metallurgical characterization of controlled memory wire nickel-titanium rotary instruments. *J Endod* 2011;37:1566-71.
- Pedullà E, Ambu E, Rovai F, et al. Influence of proper or reciprocating optimum torque reverse kinematics on cyclic fatigue of four single files. *J Investig Clin Dent* 2019;10:e12409.
- Hülsmann M. Research that matters: studies on fatigue of rotary and reciprocating NiTi root canal instruments. *Int Endod J* 2019;52:1401-2.
- Silva EJNL, Martins JNR, Lima CO, et al. Mechanical tests, metallurgical characterization, and shaping ability of nickel-titanium rotary instruments: A Multi-method Research. *J Endod* 2020;46:1485-94.